EPS-HEP 95 Ref. eps0527
Submitted to Pa 19
Pl 6

DELPHI 95-67 PHYS 502
30 June, 1995

Upper limits on the branching ratios $\tau \to \mu\gamma$ and $\tau \to e\gamma$

DELPHI Collaboration

Paper submitted to the "EPS-HEP 95" Conference
Brussels, 27th July-2nd August 1995

EPS-HEP 95 Ref. eps0527
Submitted to Pa 19
Pl 6

DELPHI 95-67 PHYS 502
30 June, 1995

Upper limits on the branching ratios $\tau \to \mu\gamma$ and $\tau \to e\gamma$

Preliminary

DELPHI Collaboration

Abstract

The DELPHI collaboration has searched for lepton flavour violating decays $\tau \to \mu\gamma$ and $\tau \to e\gamma$ using a data sample of about 70 pb^{-1} of integrated luminosity corresponding to 81 000 produced $\tau^+\tau^-$ events. No candidates were found for either of the two modes. This yields branching ratio upper limits of $B(\tau \to e\gamma) < 1.1 \times 10^{-4}$ and $B(\tau \to \mu\gamma) < 6.2 \times 10^{-5}$ at 90% confidence level.

1 Introduction

Lepton flavour violation has never been observed in nature. In the Standard Model, however, there is no fundamental reason why lepton flavour should be conserved. Instead, conservation of lepton flavour is assured by assuming zero mass for neutrinos. For non-zero neutrino masses and mixing between neutrino flavours the Standard Model predicts very low, but non-zero, rates for decays such as $\tau \to \mu\gamma$ and $\tau \to e\gamma$. Several extensions to the Standard Model give room for larger rates. These include models with additional heavy neutrinos [1], and models of supersymmetric grand unification, where the branching ratio $B(\tau \to \mu\gamma)$ is expected to exceed $B(\mu \to e\gamma)$ by five orders of magnitude [2]. Models which are symmetric with respect to left- and right-handed leptons can accomodate rates which are within reach given current experimental possibilities [3].

At LEP τ leptons are produced through the reaction $e^+e^- \to Z^0 \to \tau^+\tau^-$ at a centre of mass energy on or close to the Z^0 mass. The τ pairs are cleanly separated from $q\overline{q}$ events through the low multiplicity of the decay products, and from electron and muon pairs through the energy carried away by the undetected neutrinos. In the following a search for the two decay modes $\tau \to \mu\gamma$ and $\tau \to e\gamma$ is presented. The main signatures of these decay modes are that all the energy of the initial τ should be seen, and that the invariant mass of the observed decay products should equal the τ mass. The data sample used was collected by the DELPHI experiment from 1990 through 1993 and corresponds to an integrated luminosity of about 70 pb^{-1}.

2 Detector description

The DELPHI detector is a general purpose detector with a magnetic field of 1.2 Tesla provided by a large superconducting solenoid. The principal detector components used in this investigation were the tracking devices for track and momentum reconstruction, the electromagnetic calorimeters for electron and photon identification, and the hadron calorimeters and muon chambers for muon identification. The main tracking device was the Time Projection Chamber (TPC) which is a large drift chamber extending over radial distances R from 35 to 111 cm. The tracking was supplemented by the Vertex Detector (VD), the Inner Detector (ID) and the Outer Detector (OD) to reconstruct charged particle tracks at large angles to the beam axis. For particles emerging at smaller angles, the forward drift chambers (FCA and FCB) supplemented the TPC for track reconstruction. The electromagnetic calorimetry consisted of an array of lead glass blocks (FEMC) in the polar angular regions $0.804 < |\cos\theta| < 0.985$ and of the High density Projection Chamber (HPC) for $|\cos\theta| < 0.73$. The HPC was radially segmented into 9 layers, and was built up of a total of 144 modules. The hadron calorimeter (HCAL) was radially segmented into 4 layers and covered 98% of the solid angle. For muon detection, chambers were placed between the third and the fourth HCAL layer and outside the fourth layer, covering nearly the same solid angle. A detailed description of the DELPHI detector can be found in [4].

3 Preselection of $\tau^+\tau^-$ pairs

Starting with events with a multiplicity of $2 \leq N_{ch} \leq 6$, the charged particle tracks were divided into hemispheres by a plane perpendicular to the event thrust axis. The

highest momentum particle in at least one of the hemispheres should have a polar angle satisfying $|\cos\theta| < 0.94$. The main criteria for preselecting $\tau^+\tau^-$ pairs from Z^0 decays took advantage of the fact that in a standard τ decay a substantial part of the energy is carried away by the neutrino(s), or by the γ in the modes which were sought in this analysis. In order to preserve efficiency when neutral particles carry little energy, the neutral or missing energy in both hemispheres was taken into account simultaneously. The variable $P_{rad} = \sqrt{P_1^2 + P_2^2}$, where P_1 and P_2 are the momenta of the leading particle in hemisphere 1 and 2 respectively, was particularly useful. Similarly, to remove e^+e^- pairs, a variable $E_{rad} = \sqrt{E_1^2 + E_2^2}$ was defined using the electromagnetic energies associated to the leading charged particle. Another characteristic of the τ decay products observed in the detector is that they, contrary to e^+e^- and $\mu^+\mu^-$ pairs from Z^0 decays, are expected to be acollinear, the acollinearity is defined as 180° minus the angle between the resultant momentum vectors from each hemisphere.

Events in which at least one particle had $|\cos\theta| < 0.73$ should satisfy the conditions $P_{rad} < P_{beam}$ and $E_{rad} < E_{beam}$, where P_{beam} and E_{beam} denote the beam momentum and energy. Furthermore a minimum acollinearity of 0.5° was imposed for events with only one charged particle per hemisphere. For events where all particles had $|\cos\theta| > 0.73$ these cuts were tightened by requiring $P_{rad} < 0.9 \times P_{beam}$ and $E_{rad} < 0.9 \times E_{beam}$, and the acollinearity for events with two charged particles was required to exceed 2°.

To reduce the background from $\gamma\gamma$ events and cosmic rays the following requirements were imposed for all events: A minimum visible energy of $0.2 \times E_{beam}$ was demanded. To suppress cosmic muons, the distance of closest approach of the leading tracks to the nominal interaction point was required to be less than 1.5 cm in the Rϕ plane and less than 4.5 cm in the z coordinate. A minimum transverse momentum for the event of 0.4 GeV/c was also imposed, a requirement which suppressed $\gamma\gamma$ events.

4 Particle identification

As a first step, τ decay candidates with more than one charged particle were rejected. A minimum momentum of 2 GeV/c on the single particle was also required.

The electron identification was restricted to charged particles in the region $|\cos\theta| < 0.71$. This is well within the angular coverage of the HPC and electrons are thus expected to deposit all its energy in the HPC. Requiring the ratio $E_{HPC}/E_{track} > 0.5$ selected electrons with high efficiency. Here E_{HPC} is the energy deposit in the HPC and E_{track} is the particle energy inferred from the momentum measurement. Furthermore, the leakage of shower energy into the hadron calorimeter should not exceed 1 GeV.

Muons could be identified both from the muon chamber response and from the response of the hadronic calorimeter. Only tracks with an energy deposit in the electromagnetic calorimeters (HPC and FEMC) of less than 1.5 GeV were considered. The hit information in the muon chambers was used by performing a fit of the extrapolated track to the hits in the chambers, retaining candidates passing the fit. The response from the HCAL was required to be compatible with a minimum ionising particle (mip). After normalising the HCAL energy deposit to the equivalent deposit at normal incidence, the compatibility was ensured by requiring a total energy deposit in the HCAL larger than 1 GeV, including more than 200 MeV in the outermost layer, and an average energy deposit per layer less than 3 GeV. If the reconstructed polar angle of the muon candidate was such that

$|\cos\theta| < 0.71$ it was accepted as a muon if it passed either the muon chamber analysis or the HCAL analysis. For events where both leading particles had $|\cos\theta| \geq 0.71$, muon candidates had to satisfy both requirements.

For each hemisphere, the most energetic cluster found in the electromagnetic calorimeters and not associated to a charged particle track was retained for further analysis provided it had an energy above 1 GeV. If the neutral was found in the HPC, a deposition of energy of at least 200 MeV in at least two consecutive layers was required. To suppress photons from bremsstrahlung in the detector, the reconstructed shower axis was required to agree to within 10° with the direction expected for a photon coming from the interaction point.

5 Simulation

Kinematically, $\tau \to \mu\gamma$ and $\tau \to e\gamma$ decays are almost identical to the mode $\tau \to \pi\nu_\tau$ at LEP energies. The $\pi\nu_\tau$ mode has an angular distribution of

$$W(\theta^*) = \frac{1}{2}(1 + P_\tau \cos\theta^*) \tag{1}$$

where P_τ is the τ polarisation and θ^* is the emission angle in the τ rest frame. The most general form for the modes sought can be written

$$W(\theta^*) = \frac{1}{2}(1 + AP_\tau \cos\theta^*) \tag{2}$$

with $-1 \leq A \leq 1$. $A = 1(-1)$ corresponds to only left-handed (right-handed) photon helicity in the decays.

A total of 6000 τ pair events were generated with an $e\gamma$ or $\mu\gamma$ final state in one hemisphere by using the KORALZ [5] event generator. The second τ in the event was required to decay into one of its standard modes in agreement with the known properties of the τ . In order to study systematic effects, half of the events were generated with $A = 1$ and the other half with $A = -1$. The events were tracked through the detector using a full simulation of the DELPHI detector, and subsequently reconstructed with the same program as the real data.

6 Selection of $e\gamma$ and $\mu\gamma$ candidate events

If the decays $\tau \to \mu\gamma$ and $\tau \to e\gamma$ did take place, all the initial energy of the decaying τ should have been seen in the detector. Furthermore, the invariant mass of the lepton photon system, $m_{l\gamma}$, should equal the τ mass. Some correlation is observed between energy and mass, and it was convenient to study the data in the variables defined by:

$$E' = (E_{l\gamma} - E_{beam})\cos\alpha + \left(m_{l\gamma}c^2 - m_\tau c^2\right)\sin\alpha \tag{3}$$

and

$$m' = \left(m_{l\gamma}c^2 - m_\tau c^2\right)\cos\alpha - (E_{l\gamma} - E_{beam})\sin\alpha, \tag{4}$$

For an appropriate choice of α, the distribution in m' can be made symmetric, while the E' distribution appears with a tail towards low values. The optimal value of the

rotation angle α was determined to be $\alpha = 2.2°$. This gave the highest signal efficiency, when defining a preliminary contour for the signal region. For simulated $\tau \to \mu\gamma$ events, the m' distribution had a standard deviation of .09 GeV, and the central part of the E' distribution had a standard deviation of 2.04 GeV. A signal region consisting of the area within the 2.5 σ contour was defined. This requirement is formulated by defining a variable R given by the equation

$$R = \sqrt{\left(\frac{E'}{5.1GeV}\right)^2 + \left(\frac{m'}{0.23GeV}\right)^2} \tag{5}$$

which should be less than unity for candidate events. The corresponding $\tau \to e\gamma$ distributions had a similar width in m', but the E' distribution had a much more pronounced tail. Since more background is expected in this channel, the signal region was not redefined to include more of this tail. Instead, the $\tau \to \mu\gamma$ contour was used to define the signal region also in the $\tau \to e\gamma$ search. Figures 1a) and b) show the reconstructed energy versus invariant mass for simulated events with the contour ellipse superimposed. In figures 2 and 3 the distributions of the variable R are displayed for the simulated signal events and for all the data. The distributions of R are shown for the events reconstructed, and for those events which remain after rejecting background as described below.

Important sources of background were e^+e^- and $\mu^+\mu^-$ pairs, with one or more extra photons present. Most of these were removed by requiring that the total energy in the hemisphere opposite to candidate events should be less than 80% of the beam energy. All events with a muon candidate in each hemisphere were removed from the search if both reconstructed particle tracks satisfied $|\cos\theta| > 0.73$. For events with at least one particle in the range $|\cos\theta| < 0.73$ and a muon candidate in both hemispheres, P_{rad} was required to be less than $0.8 \times P_{beam}$. In addition, special care had to be taken of events close to boundaries between detector modules. Events where one of the two leading tracks projected back to within 1.5° of the boundary between TPC modules were thus rejected. If one of the two leading tracks tracks projected in ϕ to within 1.0° of the border between two HPC modules, the E_{rad} requirement was tightened to $< 0.6 \times E_{beam}$. When the charged particle track opposite to an $e\gamma$ candidate pointed into this border region, the energy deposition in the hadron calorimeter was used to reject electrons. If the energy deposit in the first layer of the hadron calorimeter was larger than 3 GeV while no energy was deposited in the two outermost layers, the event was discarded; this suppressed the e^+e^- background further.

After applying these requirements, no events remained with $R < 1$. Figures 1c) and 1d) display the reconstructed energy versus invariant mass for $e\gamma$ and $\mu\gamma$ candidates, after being subjected to the full analysis. Although the signal region contained no events, some background might be expected. The events close to the signal region might be of two kinds. Firstly, radiative e^+e^- and $\mu^+\mu^-$ pairs could still be present. These events would satisfy the energy conservation condition, but they have a continuous spectrum of invariant masses because of the continuous spectrum the emission angle of the γ candidate with respect to the charged track. However, from a sample of simulated e^+e^- and $\mu^+\mu^-$ events corresponding to about three times the statistics in the data, no events passed the background cuts described above. The second important background consist of τ decays. These events can be leptonic τ decays with a radiated γ. $e\gamma$ candidates can also be formed from decays with one charged and one or more neutral pions. The reconstructed energies and masses resulting from these backgrounds extend into the signal region. From

a sample of simulated $\tau^+\tau^-$ pairs, the background levels expected were 0.6 ± 0.4 events for the $\tau \to e\gamma$ analysis and 0.3 ± 0.3 events for the $\tau \to \mu\gamma$ search.

7 Estimate of limits

The efficiency of the analysis was estimated from simulation and cross-checked by comparison with data. The efficiency of the electron and muon identification was cross-checked by verifying that the branching fractions of the decays $\tau \to \mu\nu\overline{\nu}$ and $\tau \to e\nu\overline{\nu}$ could be reproduced to values which were consistent with the known values [6]. The systematic uncertainties on the charged particle identification efficiency has been estimated to be slightly below 2%, and 2% was taken as a systematic uncertainty.

The photon identification efficiency was checked by the use of $\mu^+\mu^-\gamma$ events. Using the event generator DYMU3 [7] and full detector simulation, the number of reconstructed photons per event was compared to the corresponding number in the data after selecting events with a pair of muons. Energy dependence and dependence on the opening angle between the charged track and the neutral cluster was studied. Good agreement between data and simulation was observed for opening angles appropriate for this analysis. To cross-check, τ decays with the presence of photons from π° decays were used. τ decays containing electron and muon candidates were removed, and the spectrum of the most energetic photon candidate was studied. A comparison between simulation and data did not show any energy dependent discrepancy, but an overall correction factor of 0.98 ± 0.02 was deduced. Resolution effects were studied by the use of e^+e^- and $\mu^+\mu^-$ pairs. Corrections to the HPC energy resolution found for electrons were also applied to photon candidates. The linearity of the energy estimate of the photon candidates was checked by using kinematically constrained $e^+e^-\gamma$ and $\mu^+\mu^-\gamma$ events. A small overestimate of the reconstructed energies could not be excluded in the data. This did not affect the $e\gamma$ efficiency notably as such an overestimate would pull more of the tail into the signal region. However, such a shift would lead to a decrease of 2% in the $\mu\gamma$ efficiency and was included as a systematic uncertainty. Other systematic effects studied include those due to the unknown momentum distribution in the events searched for due to the unknown value of A in eq. (2). These studies were done on independent samples of simulated events, and the effects were found to be small compared to the uncertainty due to the simulated event statistics.

The efficiency with respect to the full solid angle was thus estimated at $(14.6 \pm 0.8)\%$ for the $e\gamma$ final state and $(24.5 \pm 1.2)\%$ for the $\mu\gamma$ final state. Using measured cross-sections [8] and estimates of the effective integrated luminosity, the number of τ decays within the full solid angle was estimated to be 162 000. Using the 90% confidence level lower limits of the efficiencies this leads to the following upper limits:

$$B(\tau \to e\gamma) < 1.1 \times 10^{-4}$$

$$B(\tau \to \mu\gamma) < 6.2 \times 10^{-5}$$

at 90% confidence level. The $\tau \to e\gamma$ result is comparable to the ARGUS result of $B(\tau \to e\gamma) < 1.2 \times 10^{-4}$ [9]. The result on $\tau \to \mu\gamma$ is however surpassed by $B(\tau \to \mu\gamma) < 4.2 \times 10^{-6}$ from CLEO [10] which is currently the most stringent limit on that decay mode.

Acknowledgements

We are greatly indebted to our technical collaborators and to the funding agencies for their support in building and operating the DELPHI detector, and to the members of the CERN-SL Division for the excellent performance of the LEP collider.

References

[1] J.W.F. Valle, Prog. in Nucl. and Part. Physics 26 (1991) 91.

[2] R. Barbieri and L.J. Hall, Phys. Lett. B338 (1994) 212.

[3] R. N. Mohapatra, Phys. Rev. D46 (1992) 2990.

[4] DELPHI Collaboration, P. Aarnio et al., Nucl. Instr. Meth. A303 (1991) 233.

[5] S. Jadach and Z. Was, Comp. Phys. Commun. 36 (1985) 191;
S. Jadach, B.F.L. Ward and Z. Was, Comp. Phys. Commun. 66 (1991) 276.

[6] Particle Data Group, Phys. Rev. D 50 (1994) 1173.

[7] J.E. Campagne and R. Zitoun, Zeit. Phys. C43 (1989) 459; Proc. of the Brighton Workshop on Radiative Corrections, Sussex, July 1989.

[8] DELPHI Collaboration, P. Abreu et al., Nucl. Phys. B418 (1994) 403.
DELPHI Collaboration, P. Abreu et al., Zeit. Phys. C55 (1992) 555.

[9] ARGUS Collaboration, H. Albrecht et al., Zeit. Phys. C55 (1992) 179.

[10] CLEO Collaboration, A. Bean et al., Phys. Rev. Lett. 70 (1993) 138.

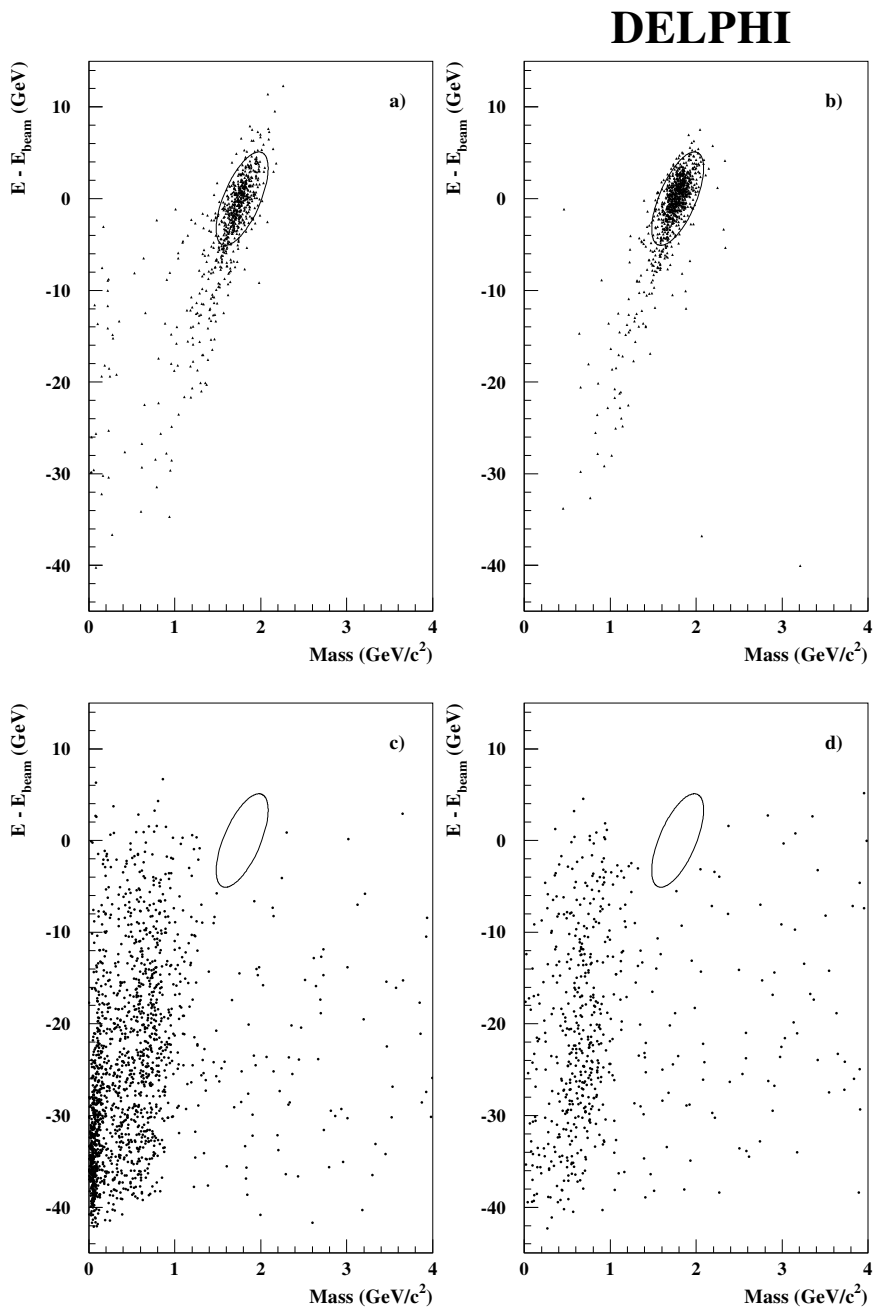

Figure 1: Reconstructed energy minus beam energy vs. invariant mass. a) Simulated $\tau \to e\gamma$ events, b) Simulated $\tau \to \mu\gamma$ events, c) $e\gamma$ candidates, d) $\mu\gamma$ candidates. The signal region was defined by the ellipse which is superimposed on the figures.

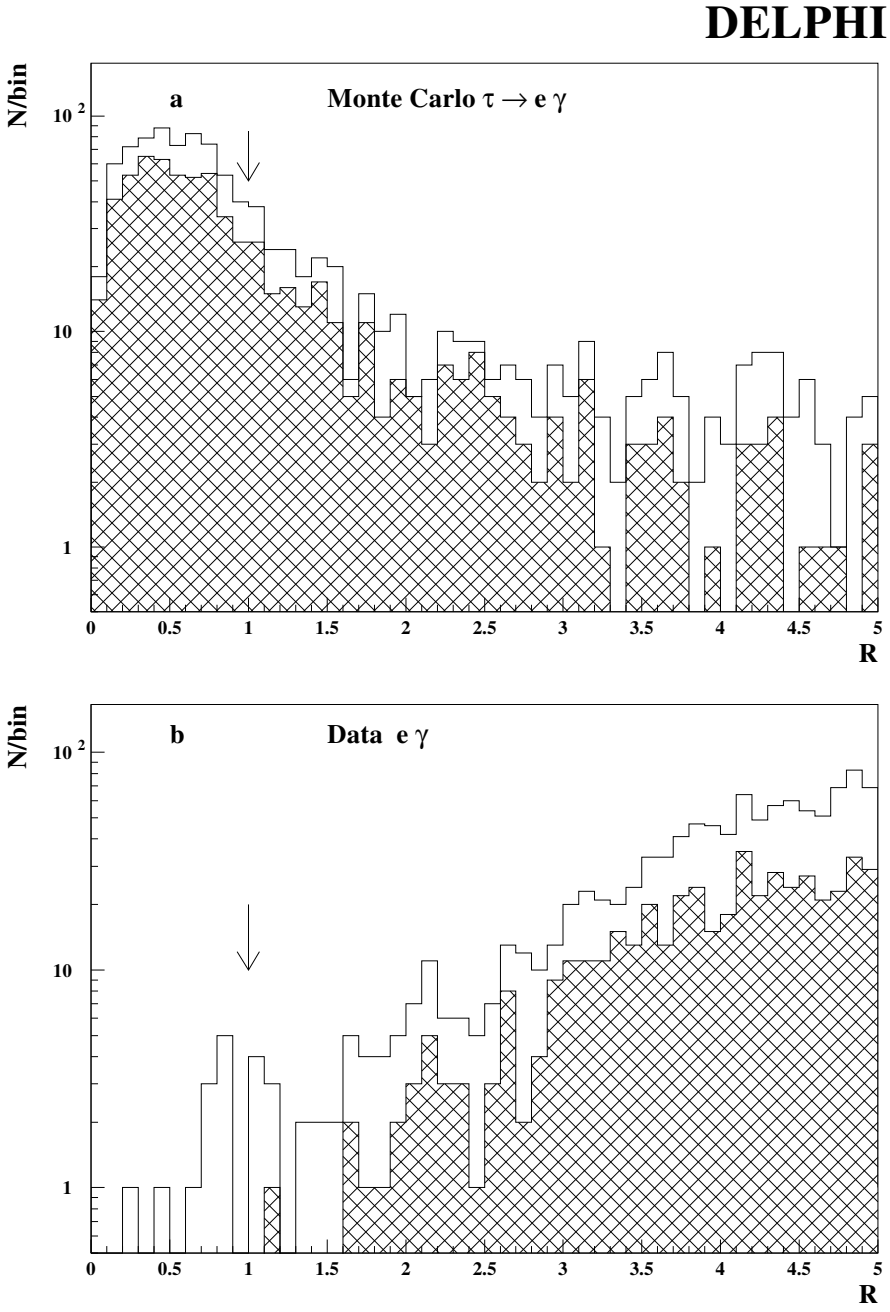

Figure 2: Distribution in the variable R for $\tau \to e\gamma$ candidates. a) Simulated events, b) data. Open histograms are before the background rejection described in the text, hatched histograms are after these cuts. No events remain in the signal region, $R < 1$. The arrows indicate the final cut.

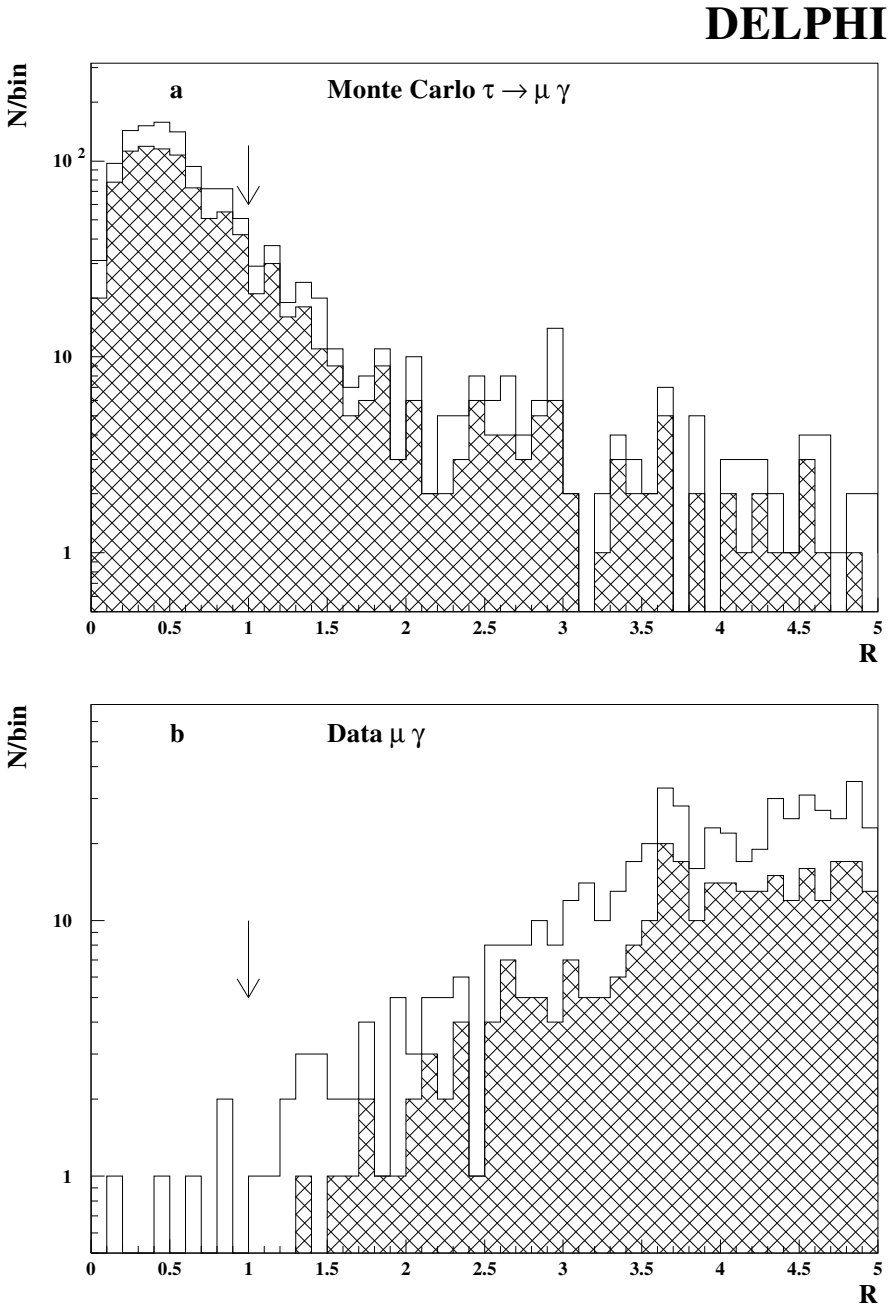

Figure 3: Distribution in the variable R for $\tau \to \mu\gamma$ candidates. a) Simulated events, b) data. Open histograms are before the background rejection described in the text, hatched histograms are after these cuts. No events remain in the signal region, $R < 1$. The arrows indicate the final cut.